Improvement of Stability of a High-Loaded Axial Flow Compressor by a Combined Flow Control Method

MENG Dejun, YIN Haibao, LIU Jie*

Shenyang Engine Research Institute, Aero Engine Corporation of China, Shenyang 110015, P. R. China

(Received 13 September 2025; revised 20 January 2026; accepted 1 March 2026)

Abstract: This study investigates a high-loaded axial compressor in which flow instabilities in the rotor and the stator occur almost concurrently. Under these conditions, conventional stability enhancement methods prove to be ineffective. The paper proposes a combined rotor-stator flow control technique. This study reveals that the flow field deterioration stems from combined flow blockage at the rotor tip region and the near-hub region of the stator. Research on flow control methods finds that self-recirculating casing treatment can effectively improve flow capacity in the rotor tip region, but simultaneously reduce flow capacity in the near-hub zone. This makes the hub flow field more susceptible to breakdown and ultimately triggers compressor instability. Thus, the self-recirculating casing treatment fails to enhance stall margin. By contrast, hub suction significantly improves the hub-region flow field. Yet without suppressing the rotor-tip flow blockage, it achieves limited stability enhancement. The integrated solution combining self-recirculating casing treatment with hub suction simultaneously addresses flow blockage at both the rotor tip and the stator near-hub regions. This combined flow control method delivers effective stability enhancement, achieving 6.78% increase in compressor stall margin.

Key words: axial flow compressor; high load; stability; combined flow control method; flow mechanism

CLC number: V231 **Document code:** A **Article ID:** 1005-1120(2026)02-0286-15

0 Introduction

With the development of aero-engines toward higher thrust-to-weight ratios, compressor design has been increasingly oriented toward fewer stages and higher pressure-ratios. This trend inevitably leads to elevated compressor stage loading. Increased stage loading intensifies the adverse pressure gradients within the compressor, resulting in more complex internal flow structures and posing significant challenges to flow stability[1-2]. Therefore, addressing flow stability issues under high-loaded conditions is critically important, particularly in enhancing the stall margin of high-loaded compressor. To this end, the development of effective flow control techniques which regulate the internal flow of high-loaded compressors plays a vital role in improving compressor stall margin.

Currently flow control methods include casing treatments, tip injection, end-wall contouring, boundary layer suction, and vortex generators, etc[3-15]. Among these, casing treatments have garnered significant attention in the turbomachinery research field due to their structural simplicity, ease of implementation, and pronounced effectiveness in enhancing stability. Existing studies have shown that among various casing treatment methods, circumferential grooves offer relatively weak stall margin enhancement and minimal adverse effects on compressor efficiency[16-18]. In contrast, slot-type casing treatments provide stronger stability improvement, albeit often at the cost of substantial efficiency losses[19-21]. Compared to the above two methods, self-recirculating casing treatments strike a better bal-

*Corresponding author, E-mail address: 154513049@qq.com.

How to cite this article: MENG Dejun, YIN Haibao, LIU Jie. Improvement of stability of a high-loaded axial flow compressor by a combined flow control method[J]. Transactions of Nanjing University of Aeronautics and Astronautics, 2026, 43(2): 286-300.

http://dx.doi.org/10.16356/j.1005-1120.2026.02.009

ance by significantly improving stall margin while imposing relatively smaller penalties on efficiency, though they typically require a larger radial footprint[22-24]. In terms of the mechanisms through which casing treatments influence the internal compressor flow field, these three casing treatments are effective in suppressing tip leakage flow, which is a major contributor to tip-region flow deterioration. However, for tip flow deterioration caused by suction-side separation near the blade tip, circumferential grooves and slot-type treatments have limited mitigation capability. In contrast, self-recirculating casing treatments, owing to their combined suction and injection mechanisms, have demonstrated the ability to alleviate this type of flow separation-induced degradation[25]. Additionally, boundary layer suction has proven to be effective in mitigating flow separation on the blade surface and the end-wall, thereby improving overall compressor aerodynamic performance[26-28].

To ensure that compressors maintain both aerodynamic performance and stability under increasing stage loading, the design of high-loaded compressors requires refined control of inter-stage matching, leakage flows, and end-wall region flows[29-30]. Such refined designs often lead to stage loading limits that are closely matched across multiple stages. Consequently, when flow instability occurs, flow deterioration tends to emerge almost simultaneously across multiple blade rows. For instance, in the 1.5-stage high-loaded axial compressor investigated in this study, flow deterioration is observed both at the rotor tip of the first stage and near the hub of the first stator during the onset of flow instability. In such cases, applying flow control to a single region, either the rotor tip or the stator hub, fails to significantly enhance the compressor stall margin. This necessitates the exploration of new flow control methods. When flow deterioration originates from multiple locations within the compressor, or when a single flow control technique is insufficient to address the complex flow issues, combined flow control methods become an effective solution to improve the internal flow field. Du et al.[31] and Li et al.[32] conducted experimental and numerical studies on a combined front-slot and rear-groove casing treatment in a low-speed axial compressor. Compared with full-slot and full-groove casing treatments, their results showed that the combined design offered a stall margin enhancement and peak efficiency loss that were intermediate between the two individual methods. The combined casing treatment improved the stall margin by reducing blade loading and weakening tip leakage flow and its associated unsteady disturbances. Liu et al.[33] carried out similar experimental and numerical investigations on a high-speed axial compressor at Northwestern Polytechnical University and reached comparable conclusions. Wang et al.[34] studied a high-loaded 2.5-stage transonic compressor. They found that compressor stall was not triggered by tip leakage flow but by boundary layer separation induced by strong tip shock waves. This type of stall was identified as a tip-overload stall, i.e., a subtype of spike stall. Experimental results showed that conventional casing treatments failed to enhance the stability margin of this compressor. To address this, a novel casing treatment combining self-recirculating and slot-type features was proposed. Numerical investigations demonstrated that this combined casing treatment could effectively improve the compressor stall margin, although it also shifted the stall inception location to the stator. Zhang et al.[35] studied three flow control methods combining blade slotting with boundary layer suction. Their findings indicated that all combined methods significantly extended the stall margin compared to single flow control methods. At the near-stall conditions, the partial-span slotting case showed lower total pressure loss and higher efficiency than full-span slotting case. Notably, the upper-half slotting configuration achieved the highest stall margin, validating the feasibility of blade slotting combined with boundary layer suction as a combined flow control method.

In summary, various flow control methods improve the stall margin of compressors by enhancing the internal flow field. However, there is limited research on stability enhancement methods for high-loaded compressors, particularly for those where flow instability is almost simultaneously triggered across multiple blade rows. Research on such stability improvement techniques for high-loaded compressors with nearly simultaneous flow instability across rotor tip and the stator hub regions is almost nonexistent. Therefore, this study focuses on a high-loaded compressor with a loading coefficient of 0.56 and a tip Mach number of 2.0, where internal flow instability is nearly simultaneously triggered at the rotor tip and the stator hub regions. This paper combines self-recirculating casing treatment, which has a minimal impact on compressor efficiency, with the boundary layer suction technology. Thus, it adopts a combined flow control method to improve the stability of this high-loaded compressor. This study also analyzes the underlying mechanisms of various flow control methods on the internal flow field of the compressor. The results will provide theoretical insights for the stability enhancement design of high-loaded compressors.

1 Research Object and Numerical Methods

The object of this study is a 1.5-stage high-loaded axial compressor, which consists of an inlet guide vane (IGV), a first-stage rotor, and a first-stage stator. The local Mach number of the flow at the rotor tip inlet reaches as high as 2.0. Fig.1 shows a schematic diagram of the computational domain for the compressor in this study, which is composed of the inlet domain, the inlet guide vane domain, the rotor domain, the stator domain, and the outlet domain. The grid topology for the inlet guide vane, the rotor, and the stator sections is of the H-O-H type, with a butterfly-shaped grid topology for the tip gap. The first layer of grid thickness is 0.005 mm, and the y^+ value is less than 5. The radial grid point number for all sections is 97, while the axial and the circumferential grid point numbers are determined based on the axial length and the circumferential width of each section. The radial grid point numbers for the rotor and the stator tip gaps are 21 and 33, respectively. The total number of grid cells across all computational domains is approximately 3.5 million, with each blade row channel containing over 1 million grid points on average.

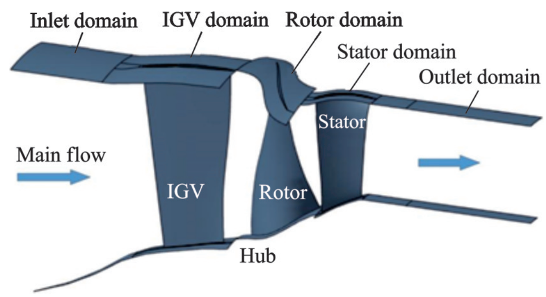

Fig.1 Schematic diagram of the computational domain for the compressor

In the numerical computations, the Spalart-Allmaras (S-A) turbulence model is employed, using a central difference scheme. Multigrid iteration techniques are used to accelerate the convergence of the solution. Between the inlet guide vane and the rotor, a one-dimensional no-reflection method is used for the rotor-stator interface, while a mix-plane method is applied between the rotor and the stator. The boundary conditions are as follows: (1) The total temperature and total pressure are specified at the inlet, with an axial flow direction; (2) the average static pressure is specified at the outlet; (3) the walls are treated as adiabatic, no-slip boundaries. The calculation is considered converged when the inlet and outlet flow, the total pressure ratio, and the efficiency either remain constant or exhibit regular periodic fluctuations within a certain range. The compressor performance curve is obtained by gradually increasing the outlet static pressure, with a precision of 100 Pa at near-stall conditions.

Since experimental testing has not yet been conducted on this high-loaded axial compressor, it is not possible to validate the numerical method using experimental data. Therefore, the NASA Rotor 37 transonic rotor is used to validate the numerical approach employed in this study. The study calculates the results using three turbulence models (S-A, k-ε, and shear stress transport (SST) models) and compares the numerical results at 100% speed with the experimental data. Fig.2 shows the total performance curves of the compressor which are calculated using different turbulence models under the same grid. From Fig.2, it is evident that all three turbulence models show certain degrees of error when compared to the experimental results, but the overall error remains within 2%. The predicted choked mass-flow rate for all three models is almost identical to the experimental results, with relative errors within 0.2%. However, in terms of predicting the near-stall mass flow rates, the S-A turbulence model provides the closest results to the experimental data, whereas the k-ε and SST models show significant deviations. Since the primary focus of this study is on the compressor stall margin, accurately predicting the near-stall mass flow rate is crucial. Based on this, the S-A turbulence model is selected for further numerical investigation in this study.

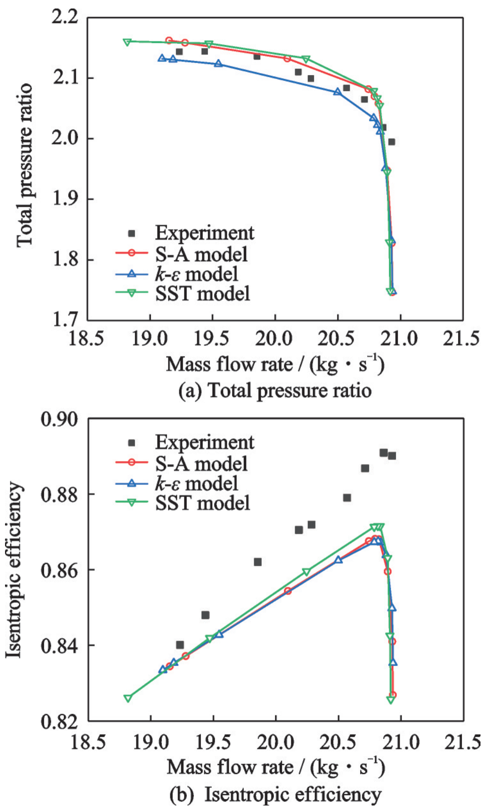

Fig.2 Compressor performance curves for different turbulence models

A limitation of this study is that since experimental tests for the current highly loaded compressor have not yet been conducted, it is not possible to validate the numerical methods with experimental data. Therefore, the accuracy of the numerical method is verified using the NASA Rotor 37 case. This is considered sufficient to meet the research objective of this paper, since it is to explore the underlying flow mechanisms and the effectiveness of the proposed combined flow control strategy through numerical simulations. Experimental validation will be performed in our future work. In addition, a grid independence study is performed to ensure that the numerical solutions are insensitive to mesh resolution. Three different grid densities are generated for the single-stage compressor, with total grid numbers of approximately 1.6 million, 3.5 million, and 4.6 million. The overall performance curves in Fig.3 indicate that the results from the 1.6 million grid noticeably deviate from the finer meshes. Specifically, it underestimates the total pressure ratio, the isentropic efficiency, and the near-stall mass flow rate. In contrast, the performance characteristics predicted by the 3.5 million and 4.6 million grids show excellent agreement with negligible discrepancies. The relative error for the near-stall mass flow rate between these two cases is less than 0.3%, suggesting that the solution has achieved grid independence once the mesh size reaches 3.5 million. Consequently, balancing computational accuracy and cost, this study selects the grid with 3.5 million cells for numerical simulations.

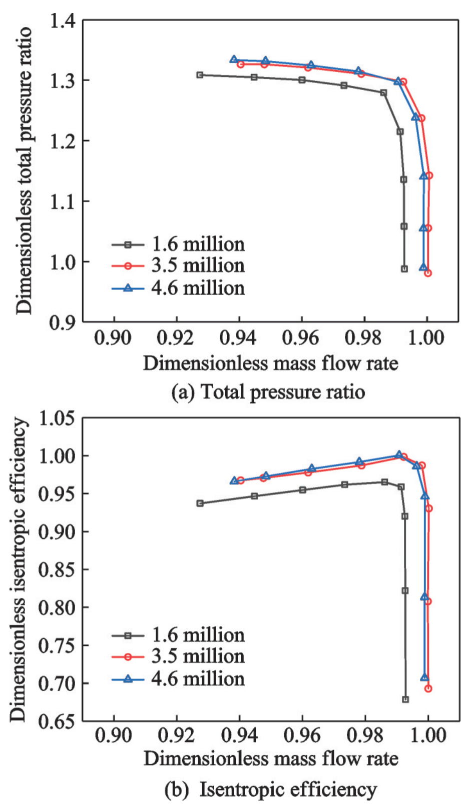

Fig.3 Compressor performance curves for different grid numbers

2 Flow Instability Mechanism of Original High-Loaded Compressor

In order to conduct stall-margin enhancement design research on this high-loaded compressor, it is essential to first fully reveal the flow instability mechanisms of the compressor. Therefore, Fig.4 presents a comparison of the changes of reflux zone in the meridional plane during the throttling process. The colored regions in Fig.4 represent the reflux zone (where $V_z<0$), and φ is the dimensionless mass flow rate calculated based on the design mass flow rate. The near-stall condition represents the final stable convergent point in the numerical simulation. Conversely, the unstable operating condition corresponds to the point immediately following near-stall along the throttling curve. As indicated by Fig.4, localized reflux zones, acting as precursors to aerodynamic degradation, are observed at both the rotor tip and the stator hub under near-stall conditions, though their scales remain relatively constrained. As throttling continues, the flow field at the unstable condition shows that the reflux zones at the rotor tip and the stator hub gradually increase in size, further inducing flow deterioration within the compressor and leading to compressor stall.

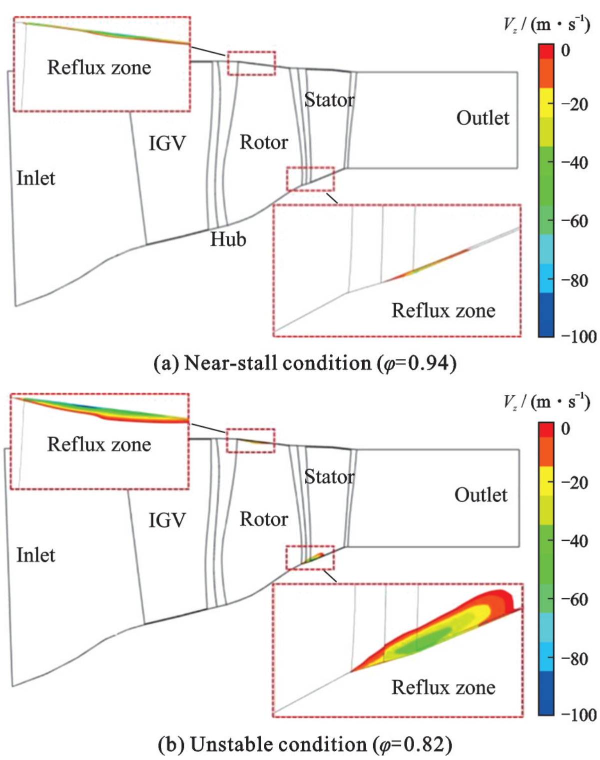

Fig.4 Comparison of reflux zone in meridional plane during throttling process

To further investigate the flow deterioration mechanisms in the rotor tip region and near the stator hub region, Fig.5 shows the flow field distribution at the rotor tip under near-stall condition, where W_{xyz} represents the three-dimensional relative velocity. It can be observed that the low-speed flow region near the leading edge of the blade and the flow separation region on the suction side are the main causes of flow deterioration at the rotor tip. The low-speed flow region near the leading edge is induced by the rotor tip leakage flow. Under the influence of these two low-speed regions, under the near-stall condition, the leading edge of the rotor tip passage is almost entirely covered by the reflux zone, which greatly restricts the flow capacity in the rotor tip region.

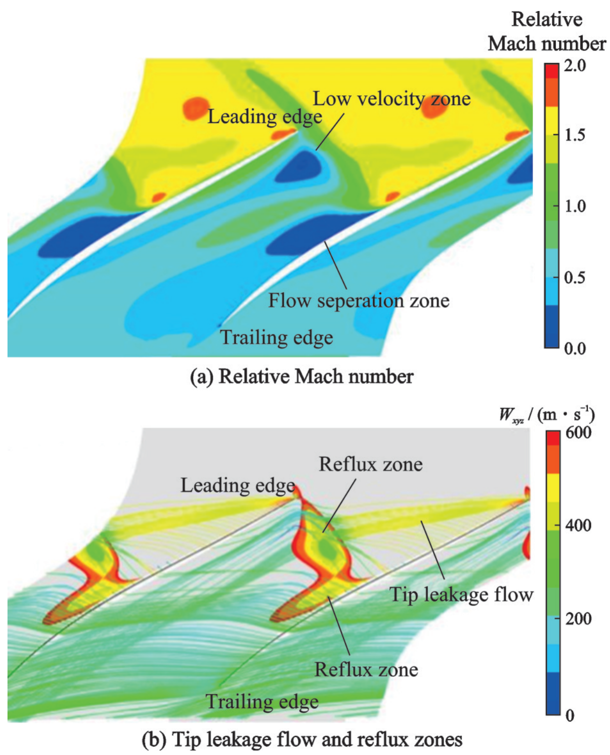

Fig.5 Distribution of flow field at rotor tip under near-stall conditions (φ=0.94)

Fig.6 presents a comparison of the flow fields in the near-hub region of the stator under both large mass flow rate and near-stall conditions. The red regions represent reflux zones (Only 0—10% span is displayed). Due to the presence of gaps at the leading edge of the stator, the pressure difference between the pressure side (PS) and suction side (SS) of the stator blade induces leakage flow through the gap. At the large mass flow rate, the incoming flow velocity is large, and the leakage flow is carried downstream by the incoming flow. In this case, the reflux zone in the stator passage is small and insufficient to induce flow deterioration, so the compressor does not stall. However, under the near-stall condition, the incoming flow velocity at the hub region decreases, and the leakage flow is less affected by the incoming flow. As a result, the leakage flow overflows at the stator leading edge (LE). Meanwhile, it can be observed that as the leakage flow moves toward the trailing edge (TE) of the stator, it gradually develops radially, which significantly worsens the flow conditions in the stator passage. At this point, the leading edge of the stator passage is filled with reflux zones, preventing the incoming flow from smoothly entering the stator passage near the hub.

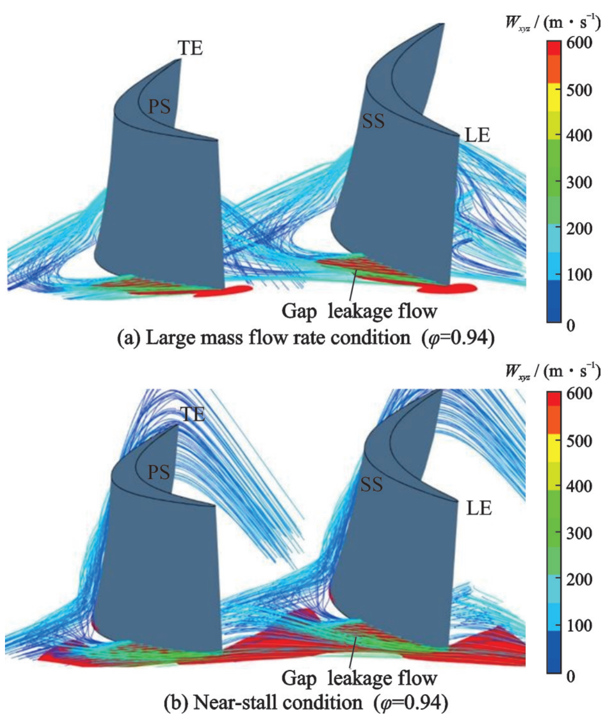

Fig.6 Comparison of flow field in near-hub region of stator under different conditions (original compressor)

Thus, it is evident that the flow conditions in both the rotor tip region and near the stator hub region significantly affect the stability of the compressor. In particular, the flow deterioration in the rotor tip region is mainly caused by rotor tip leakage flow and flow separation on the suction side, while the flow deterioration in the stator near the hub region is primarily induced by the blockage caused by stator gap leakage flow.

3 Impact of Combined Flow Control Methods on Compressor Stability

3.1 Research schemes

The self-circulating casing treatment has the characteristic of holding a minimal negative impact on compressor efficiency while improving the stability of the compressor. The boundary layer suction technique can extract low-energy fluid from the endwall region, thereby improving the internal flow field of the compressor and enhancing its performance. Therefore, in the combined flow control method, the flow control methods selected are the self-circulating casing treatment and boundary layer suction. Since this study primarily focuses on the flow mechanism, a detailed explanation of the selection process for each research method is not provided. Instead, the relevant research structures selected in previous studies are directly presented. The meridional contour of the self-circulating casing treatment is introduced in the reference[20]. The reference points for the injection and suction positions are at the rotor tip leading edge, with the upstream of the leading edge being negative and the downstream positive. The design parameters for the self-circulating casing treatment are shown in Table 1, where C_{ax} represents the axial chord length of the rotor tip.

Table 1 Basic design parameters of the compressor rotor

Parameter	Value
Injection port range	$-0.2C_{ax}$—0
Injection circumferential coverage angle/ Full annular angle	0.5
Suction port range	$0.28C_{ax}$—$0.78C_{ax}$
Suction circumferential coverage angle/ Full annular angle	0.33

Fig.7 illustrates the self-circulating casing treatment at the rotor tip. The grid for the self-circulating casing treatment is an H-type grid topology, with the grid points along the axial, radial, and circumferential directions being 221, 41, and 61, respectively. Between the grid of the self-circulating casing treatment and the rotor tip grid, two thin H-type blocks are used for numerical data transfer. A rotor-stator interface is set between these two layers of thin blocks. The frozen-rotor method is used for the rotor-stator interface in the calculation, and the other computational settings remain consistent with those of the original compressor.

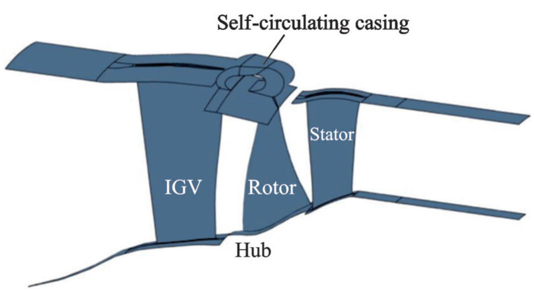

Fig.7 Schematic diagram of self-circulating casing treatment

When the compressor is operating under the near-stall condition, a reflux zone exists at the stator gap. Thus, the boundary layer suction is mainly applied in the hub region of the stator gap. Fig.8 shows the schematic of the computational domain with the boundary layer suction and the structural diagram of the suction port in the stator passage. The suction port is located in the downstream region near the stator gap, with its length and width being 8 mm and 5 mm, respectively. The center of the suction port is 12 mm downstream of the blade leading edge. The suction block uses an H-type grid, with grid points distributed in the axial, circumferential, and radial directions being 33, 25, and 161, respectively. The inlet of the suction block is connected to the hub region grid with a fully non-matching interface, and the outlet of the suction block is given an average static pressure. All other computational settings remain consistent with those of the original compressor.

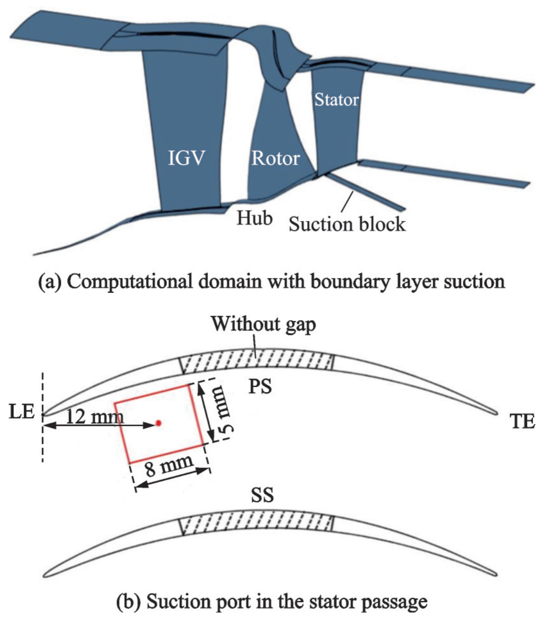

Fig.8 Schematic diagram of boundary layer suction

Furthermore, in order to improve the flow field in both the rotor tip region and the stator hub region, the self-circulating casing treatment is combined with the boundary layer suction. Fig.9 illustrates the schematic of the combined flow control method. For ease of discussion, the following abbreviations are used: Solid wall (SW) for the original compressor with solid wall casing, self-circulating casing treatment (SCT) for the compressor with self-circulating casing treatment, suction (SUC) for the compressor with boundary layer suction, and combined (COM) for the compressor with combined flow control method.

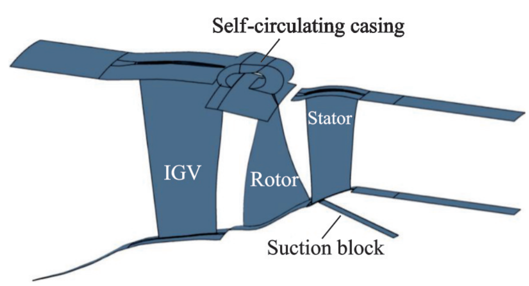

Fig.9 Schematic diagram of combined flow control method

3.2 Analysis of compressor overall performance characteristic curves

Fig.10 presents a comparison of the overall performance characteristic curves for different flow control methods. The dimensionless mass flow rate, the dimensionless total pressure ratio, and the dimensionless efficiency are dimensioned using the mass flow rate, the total pressure ratio, and the efficiency, respectively. From the comparison of the overall performance curves, it is evident that the near-stall mass flow rate for SUC and COM is lower than that of SW, indicating that these two flow control methods enable the compressor to operate stably at lower mass flow rates, thereby improving the compressor stall margin. Among these, COM exhibits a lower near-stall mass flow rate, demonstrating stronger stability enhancement ability. In contrast, the near-stall mass flow rate for SCT is higher than that of SW, suggesting that SCT does not improve the stable operating range of the compressor. In fact, the stall margin of the compressor is weakened by SCT.

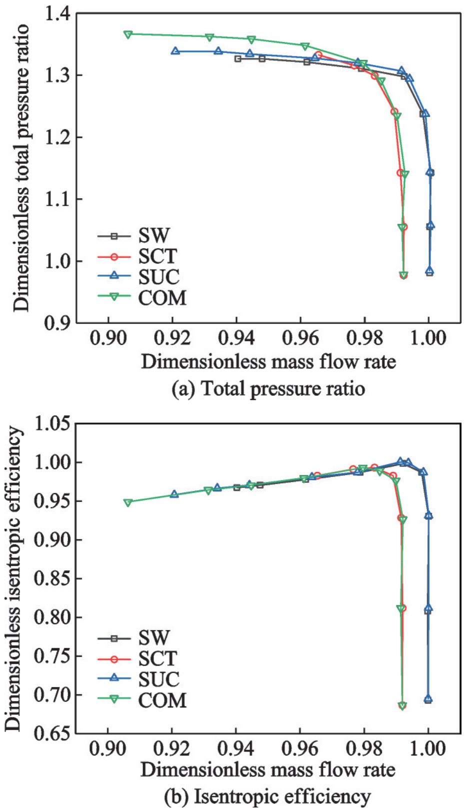

Fig.10 Compressor performance curves for different flow control methods

To quantitatively evaluate changes of the compressor stall margin, the stall margin improvement (SMI) is defined as

$$\mathrm{SMI}=\left(\frac{\pi^*_{\mathrm{NS,CT}}}{\pi^*_{\mathrm{NS,SW}}}\times\frac{\varphi_{\mathrm{NS,SW}}}{\varphi_{\mathrm{NS,CT}}}-1\right)\times 100\% \tag{1}$$

where $\pi^*_{\mathrm{NS,CT}}$ and $\pi^*_{\mathrm{NS,SW}}$ represent the dimensionless total pressure ratios at the near-stall condition for the flow control methods and SW, respectively; and $\varphi_{\mathrm{NS,CT}}$ and $\varphi_{\mathrm{NS,SW}}$ the dimensionless mass flow rates at the near-stall condition for the flow control methods and SW, respectively. If SMI is positive, it indicates that the compressor stall margin has been improved, otherwise weakened.

Table 2 compares SMI for each flow control methods. It can be observed that the self-circulating casing treatment results in a −2.37% stall margin improvement, while both the boundary layer suction and the combined flow control method enhance the compressor stall margin. Among these, the combined flow control method leads to the greatest improvement, with a 6.78% increase in the stall margin. The differences in stall margin improvement across the different flow control method will be explained in terms of the internal flow field of the compressor, revealing the flow mechanisms of each flow control methods.

Table 2 Comparison of SMI for different cases

Case	SMI/%
SCT	−2.37
SUC	2.85
COM	6.78

3.3 Flow mechanism of self-circulating casing treatment on compressor stability

The self-circulating casing treatment leads to a reduction in the compressor stall margin. To understand the flow mechanisms responsible for this phenomenon, an analysis of the internal flow field of the compressor is conducted. Since the near-stall mass flow rate for SCT is higher than that for SW, a comparison of the flow fields between SW and SCT is conducted under the near-stall mass flow condition of SCT (φ=0.96). As SCT primarily influences the rotor tip flow field, the focus is first placed on the changes in the flow field at the rotor tip. Figs.11, 12 present a comparison of the rotor tip flow fields between SW and SCT. The results show that SCT significantly improves the rotor tip

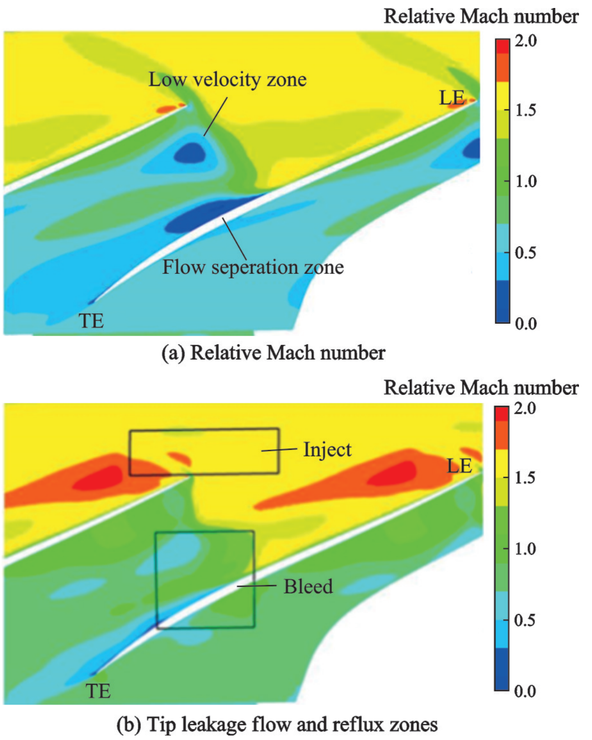

Fig.11 Comparison of relative Mach number contours at 99% span for SW and SCT (φ=0.96)

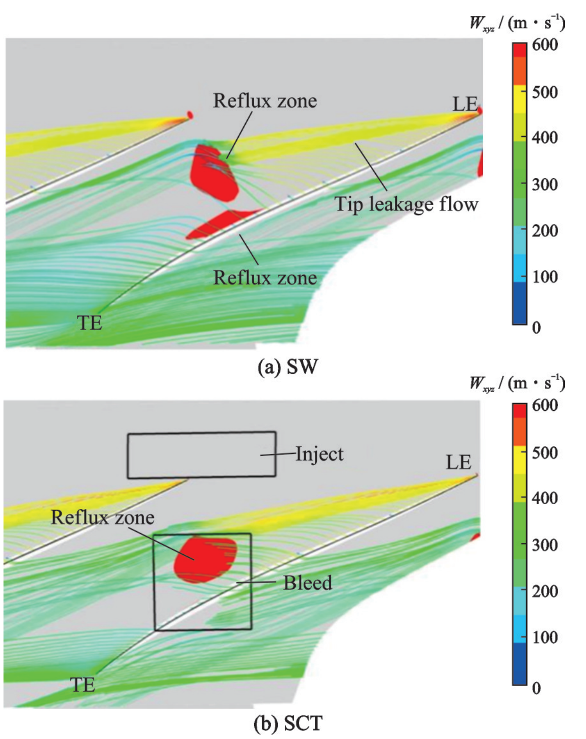

Fig.12 Comparison of tip leakage flow and reflux zone at the rotor tip for SW and SCT (φ=0.96)

flow field. Specifically, the low-speed flow regions and the flow separation zones in the tip leakage flow region and the suction side of the rotor tip are substantially reduced. The reason behind these flow field improvements lies in the enhanced inflow strength at the rotor tip due to the high-speed injected flow injected from the injection port. The increased inflow intensity causes the rotor tip leakage flow to more strongly diviate towards the suction side of the blade, thus suppressing the tip leakage flow and significantly reducing the low-speed flow regions in the trajectory of the leakage flow. Meanwhile, the suction effect at the suction port eliminates the flow separation area on the suction side of the rotor blade, improving the flow conditions on the suction side. Through the combined action of the suction and the injection port of SCT, the flow field at the rotor tip is notably improved, leading to an increase in the flow capacity of the rotor tip region.

Although SCT improves the flow capacity at the rotor tip, it does not enhance the compressor stall margin. This indicates that there are flow structures within the compressor internal flow field that are prone to triggering stall. Fig.13 presents a comparison of the meridional reflux zones between SCT and SW. Figs.13(c—d) show the flow field under unstable conditions for SCT. By comparing Figs.13(a—b), it can be observed that SCT marginally improves the flow conditions at the rotor tip, but it slightly enlarges the reflux zone in the stator near the hub region. This suggests that SCT, while improving the rotor tip flow field, makes the stator near-hub flow field more prone to deterioration. In Figs.13(c—d), as SCT continues throttling from its near-stall condition, the flow field progressively deteriorates in the stator near-hub region, while the rotor tip flow conditions remain relatively favorable. This indicates that, after SCT is applied, the stall initiation point shifts to the stator near-hub region, where the flow field deteriorates first, making it difficult for SCT to achieve effective stability enhancement.

Fig.14 shows a comparison of the flow field in the stator near the hub region between SW and SCT, where the red area represents the reflux zone. The stator blade is shown only for the 0—10% span. Fig.15 presents the comparison of the axial ve-

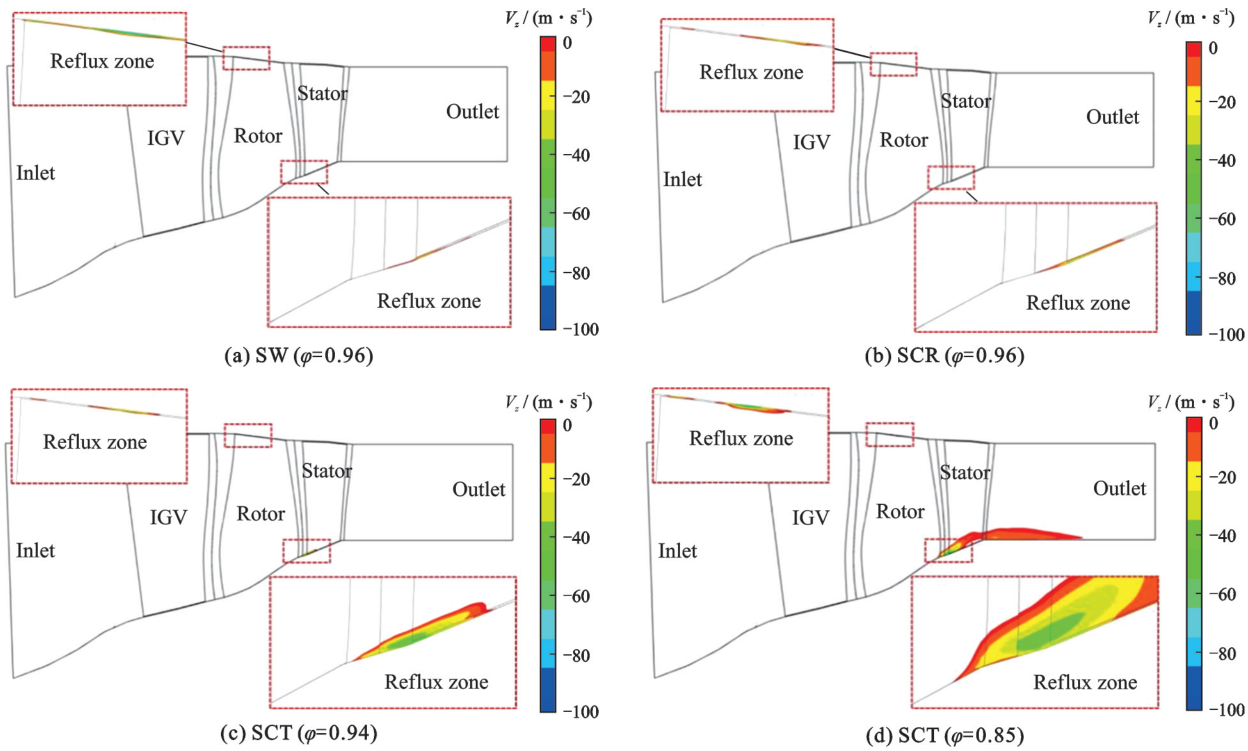

Fig.13 Comparison of reflux zone for SW and SCT in the meridional plane

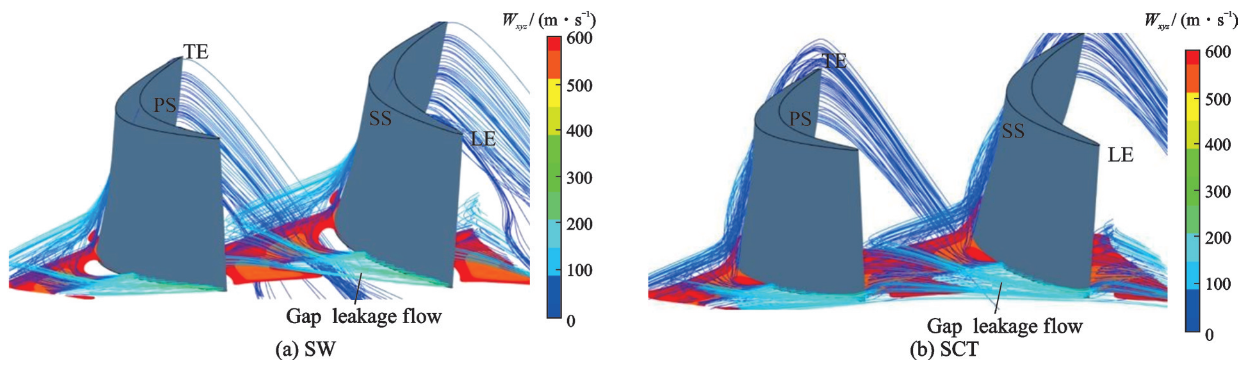

Fig.14 Comparison of flow field in the near-hub region of stator for SW and SCT (φ=0.96)

locity distribution at the stator inlet along the blade span. Compared to SW, SCT causes overflow of the stator gap leakage flow at the leading edge, and the reflux in the stator passage becomes more severe. To analyze the cause of this phenomenon, Fig.15 shows that SCT improves the flow capacity at the rotor tip region, which enhances the incoming flow velocity at the stator inlet in the rotor tip re-

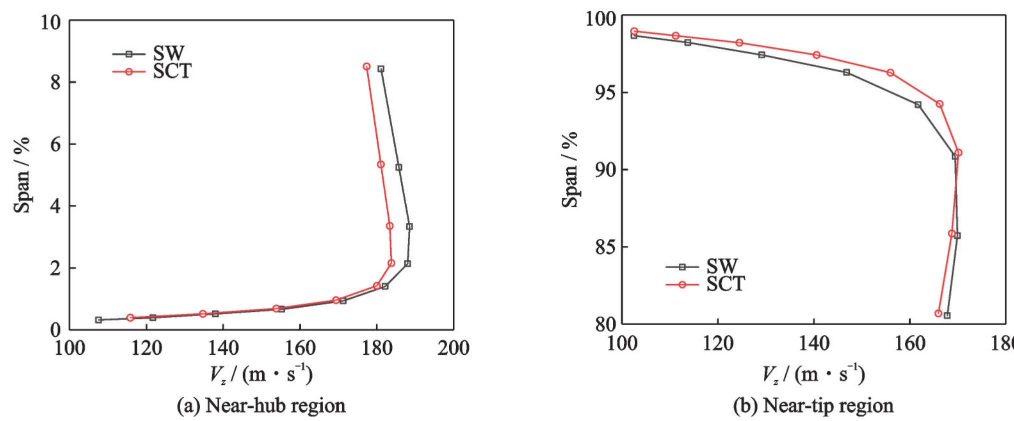

Fig.15 Comparison of stator inlet axial velocity along the blade span for SW and SCT (φ=0.96)

gion. However, as the flow capacity at the rotor tip is increased, the airflow is biased toward the rotor tip region, resulting in a decreased incoming flow velocity in the near-hub region. Consequently, the stator gap leakage flow is less influenced by the incoming flow. As a result, after applying SCT, the leakage flow at the leading edge of the stator blade overflows first, worsening the flow field in the stator near-hub region and making the compressor more susceptible to stall. This explains why SCT does not enhance the compressor stall margin, although it improves the rotor tip flow field.

3.4 Flow mechanism of boundary layer suction on compressor stability

Fig.16 shows the flow field distribution at the near-stall condition of SW for SUC. Fig.17 shows the flow field distribution at the near-stall condition for the same SUC. In Fig.16, it can be observed that the suction on the stator hub pressure side can effectively remove the stator gap leakage flow. This suction effect significantly improves the flow field in the stator near-hub region, and the reflux zone in the hub region is nearly eliminated in the meridional view. However, it is also evident that the rotor tip flow field does not grow, as reflux zones caused by

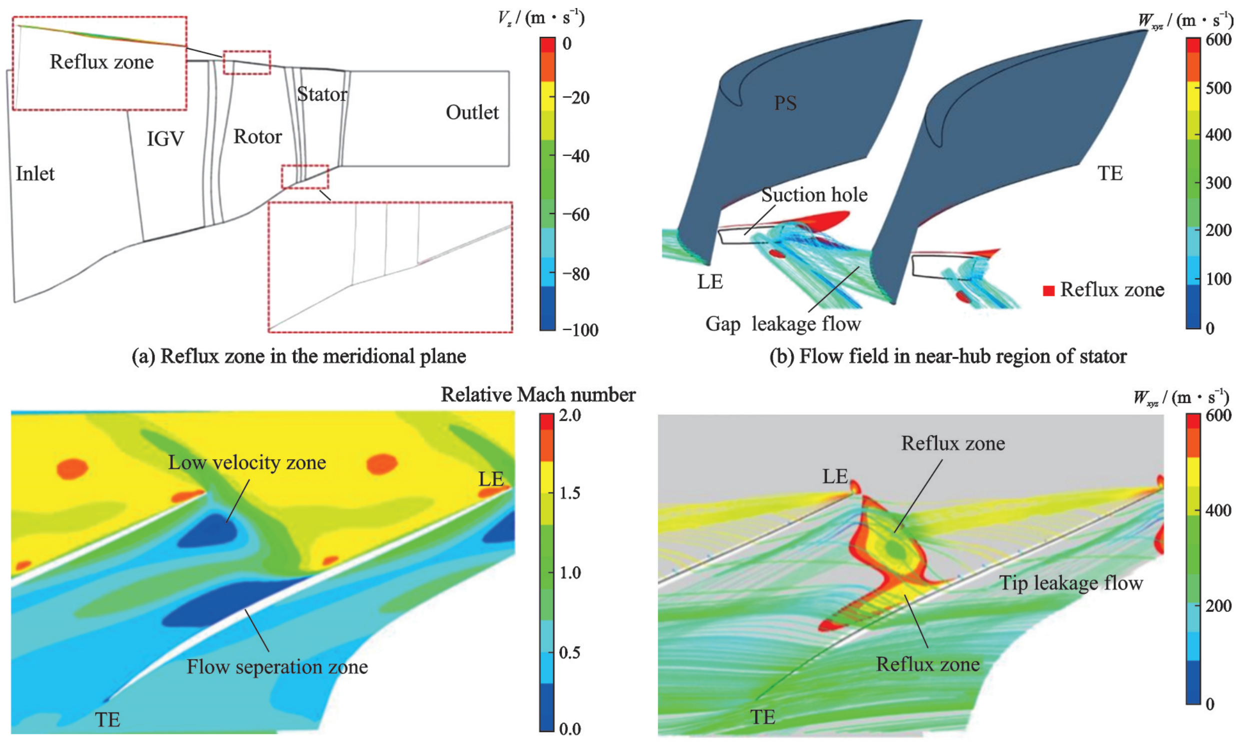

(a) Reflux zone in the meridional plane (b) Flow field in near-hub region of stator

(c) Relative Mach number contours at the rotor tip (d) Tip leakage flow and reflux zone

Fig.16 Flow field for SUC under near stall condition of SW (φ=0.94)

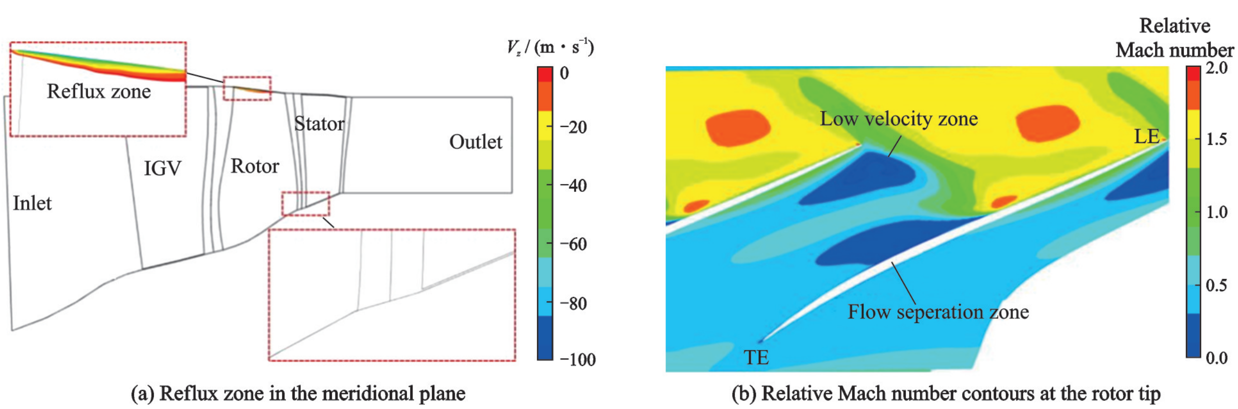

(a) Reflux zone in the meridional plane (b) Relative Mach number contours at the rotor tip

Fig.17 Flow field for SUC under near stall condition of SW (φ=0.92) tip leakage flow and suction side flow separation still exist. These reflux zones continue to impede the incoming flow at the rotor tip, presenting a potential risk of instability in the compressor's internal flow field. It can be seen from Fig.17(a) that the reflux zone in the stator near-hub region has been eliminated, and the reflux zone is entirely concentrated in the rotor tip region. Moreover, the size of this reflux zone is larger compared to the near-stall condition of SW. As shown in Fig.17(b), when compared to the rotor tip flow field at the near-stall condition for SW (Fig.16(c)), the low-speed flow region induced by the tip leakage flow in the rotor tip region becomes larger and moves toward the leading edge of the rotor tip. This further deteriorates the flow capacity of the rotor tip region. This indicates that after applying SUC, the internal flow field of the compressor deteriorates primarily due to the worsening flow conditions at the rotor tip. The reflux zone at the rotor tip is the primary cause of compressor stall, which also explains the relatively poor stability enhancement effect of SUC.

3.5 Flow mechanism of combined flow control method on compressor stability

Fig.18 shows the flow field distribution under the near-stall condition of SW for COM. After applying COM, the flow fields in both the rotor tip region and the stator near-hub region are simultaneously improved. This significantly enhances the internal flow capacity of the compressor, resulting in a substantial increase in its stall margin. From this, it can be observed that the combined flow control method not only improves the flow field at the rotor tip but also enhances the flow field at the stator near-hub region, achieving better stability enhancement effects. Therefore, when there are multiple locations in the compressor flow field that can trigger flow deterioration, the effectiveness of a single flow control method is limited, or may even fail to produce a satisfactory effect. Desired stability enhancement can only be achieved by applying one or more flow control methods that simultaneously address multiple flow field problems.

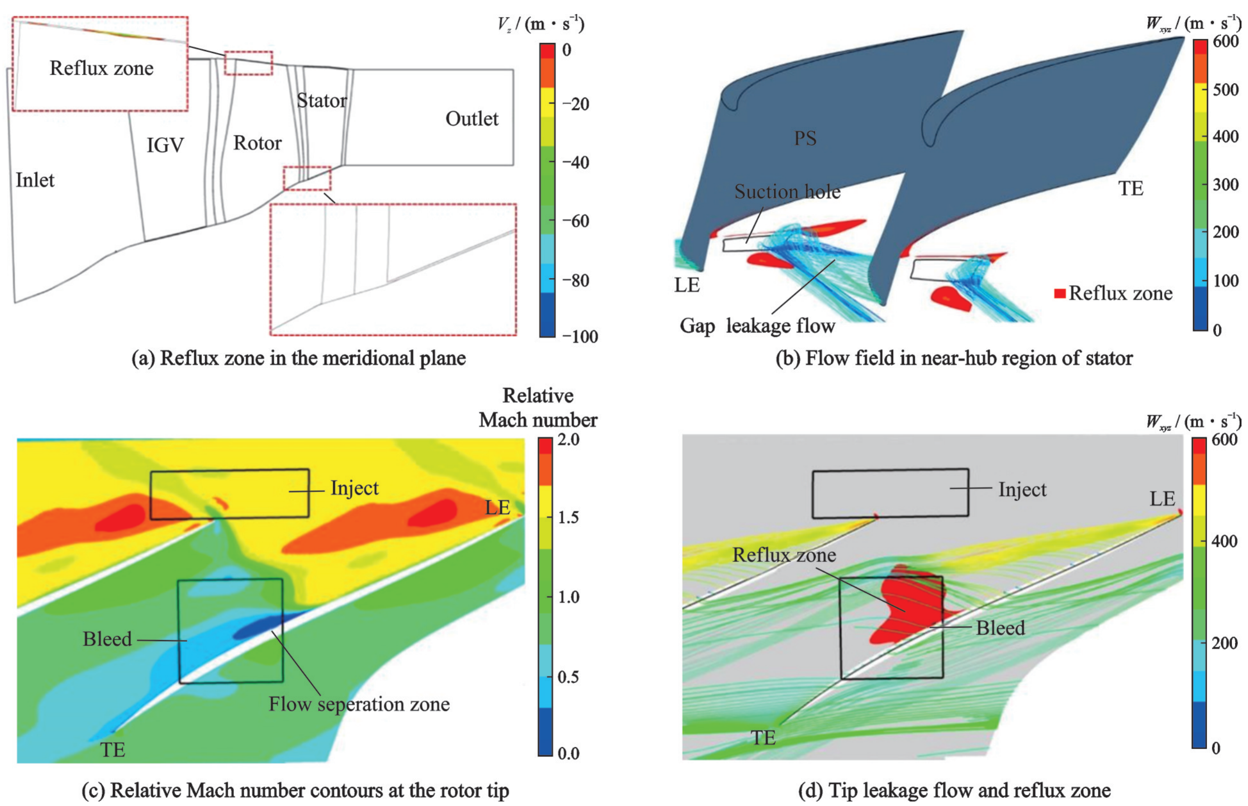

Fig.18　Flow field for COM under near stall condition of SW (φ=0.94)

4 Conclusions

This study investigates the flow mechanisms of the impact of combined flow control methods on the stability of a high-loaded axial compressor, where flow instability in both the rotor and stator occurs nearly simultaneously. The study explores the effects of both single flow control methods and combined flow control methods on the compressor's internal flow field. Through a detailed flow field comparison and analysis, the main conclusions are as follows:

(1) Flow instability in the internal flow field of the original high-loaded compressor is primarily caused by flow blockage at the rotor tip and in the stator hub region. The rotor tip flow blockage is induced by the low-speed flow area caused by tip leakage and the flow separation on the suction surface at the rotor tip. The flow blockage in the stator hub region is mainly caused by the reflux of leakage flow from the stator gap at the leading edge of the stator hub.

(2) Using the self-circulating casing treatment to improve the rotor tip flow field does not effectively enhance the stall margin of the compressor. Although the self-circulating casing treatment can effectively improve the flow capacity at the rotor tip, it causes the airflow to shift toward the tip region, which results in a reduction in the inlet velocity to the hub region. This, in turn, makes the stator hub region more prone to flow deterioration. As a result, the self-circulating casing treatment cannot effectively increase the stall margin of the compressor.

(3) Boundary layer suction at the stator pressure side near the hub can effectively suppress the development of leakage flow from the stator gap in the stator passage, thereby improving the flow capacity in the stator hub region and increasing the compressor stall margin. However, due to the lack of improvement in the rotor tip flow, flow blockage at the rotor tip continues to limit the further enhancement of the compressor stall margin. Therefore, the stabilization effect of the boundary layer suction is limited, with only a 2.85% improvement in compressor stall margin.

(4) The combined flow control method, combining self-circulating casing treatment and boundary layer suction, can effectively eliminate flow blockage at the rotor tip and in the stator hub region. This method results in a significant stabilization effect, achieving a 6.78% improvement in the compressor stall margin.

This study demonstrates the systematic efficacy of the combined casing treatment and hub modification. A key finding is that the combined approach successfully mitigates the interaction between the tip leakage vortex and the corner separation, a benefit not fully realizable by independent applications. This simultaneous suppression of blockages at both the rotor tip and stator hub constitutes the primary unique contribution of this work, offering a robust design guideline for enhancing the stability of highly loaded compressors.

This study demonstrates the aerodynamic potential of the combined flow control strategy, practical implementation faces substantial hurdles. Key challenges include the increased system complexity and energy penalty associated with the suction system. More critically, simultaneous modifications to both the hub and the casing may severely compromise the structural integrity of the compressor. Consequently, future investigations must prioritize addressing manufacturing complexity, structural strength, and overall system viability. Detailed structural analysis and experimental validation are essential to evaluate the net efficiency and real-world feasibility of this approach.

References

[1] CHEN Maozhang. Development of fan/compressor techniques and suggestions on further researches[J]. Journal of Aerospace Power, 2002, 17(1): 1-15. (in Chinese)

[2] LIU Yongquan, LIU Taiqiu, JI Lucheng. Some problems and thoughts in the development of aero-engine fan/compressor[J]. Acta Aeronautica et Astronautica Sinica, 2015, 36(8): 2563-2576. (in Chinese)

[3] NIE C Q, XU G, CHENG X B, et al. Micro air injection and its unsteady response in a low-speed axial compressor[J]. Journal of Turbomachinery, 2002, 124(4): 572-579.

[4] LI J C, LIU Y, DU J, et al. Automatic stability control using tip air injection in a multi-stage axial flow compressor[J]. Aerospace Science and Technology, 2020, 98: 105707.

[5] LIU Wenhao, CHU Wuli, ZHANG Haoguang, et al.

Experimental and numerical investigation of micro tip injection in a high-speed axial compressor rotor[J]. Transactions of Nanjing University of Aeronautics & Astronautics, 2024, 41(6): 750-765.

[6] HATHAWAY M. Passive endwall treatments for enhancing stability[D]. Ohio, USA: Glenn Research Center, 2007.

[7] NERGER D, SAATHOFF H, RADESPIEL R, et al. Experimental investigation of endwall and suction side blowing in a highly loaded compressor stator cascade[J]. Journal of Turbomachinery, 2012, 134(2): 021010.

[8] AKCAYOZ E, DUC VO H, MAHALLATI A. Controlling corner stall separation with plasma actuators in a compressor cascade[J]. Journal of Turbomachinery, 2016, 138(8): 081008.

[9] MA S, CHU W L, ZHANG H G, et al. Study of combined flow control strategies based on a quantitative analysis in a high-load compressor cascade[J]. Aerospace Science and Technology, 2019, 93: 105346.

[10] KAN X X, WU W Y, ZHONG J J. Effects of vortex dynamics mechanism of blade-end treatment on the flow losses in a compressor cascade at critical condition[J]. Aerospace Science and Technology, 2020, 102: 105857.

[11] ZHANG Jinming, SUN Dakun, LI Jia, et al. Theoretical and experimental study on SPS casing treatment with porous material[J]. Journal of Engineering Thermophysics, 2023, 44(1): 63-70. (in Chinese)

[12] ZHANG H G, LIU W H, WANG E H, et al. Effect of inverse blade angle slots on a transonic rotor performance and stability[J]. Aerospace Science and Technology, 2020, 96: 105596.

[13] LIU W H, CHU W L, ZHANG H G, et al. An optimization study of circumferential groove casing treatment in a high-speed axial flow compressor[J]. Aerospace, 2024, 11(7): 541.

[14] LI Q H, CHU W L, DONG J Z, et al. Data mining-based optimization study on T-shaped multiple groove casing treatment for axial compressor stability[J]. Physics of Fluids, 2024, 36(11): 116132.

[15] LI Q H, CHU W L, JI T Y, et al. SHAP-XGBoost enabled aerodynamic-structural balance in transonic compressors: T-shaped groove casing treatment design with data-driven parameter decoupling[J]. Aerospace Science and Technology, 2025, 164: 110391.

[16] BAILEY E E. Effect of grooved casing treatment on the flow range capability of a single stage axial-flow compressor: NASA-TM-X-2459[R]. [S.l.]: NASA, 1972.

[17] TAKATA H, TSUKUDA Y. Stall margin improvement by casing treatment: Its mechanism and effectiveness[J]. Journal of Engineering for Power, 1977, 99(1): 121-133.

[18] CHU Wuli, ZHANG Haoguang, WU Yanhui, et al. Impact of grooved width of grooved casing on stall margin improvement[J]. Acta Aeronautica et Astronautica Sinica, 2008, 29(4): 866-872. (in Chinese)

[19] CHI Zhidong, CHU Wuli, ZHANG Yaofeng, et al. Unsteady effect of slot-type casing treatment on the rotor tip flow structures in a transonic axial flow compressor[J]. Journal of Xi'an Jiaotong University, 2021, 55(11): 25-33. (in Chinese)

[20] WILKE I, KAU H P. A numerical investigation of the influence of casing treatments on the tip leakage flow in a HPC front stage[C]//Proceedings of Turbo Expo 2002, Parts A and B. Amsterdam, The Netherlands: ASMEDC, 2002, 5: 1155-1165.

[21] WILKE I, KAU H P. A numerical investigation of the flow mechanisms in a HPC front stage with axial slots[C]//Proceedings of Turbo Expo 2003, Parts A and B. Atlanta, USA: ASMEDC, 2003, 6: 465-477.

[22] HATHAWAY M D. Self-recirculating casing treatment concept for enhanced compressor performance[C]//Proceedings of Turbo Expo 2002, Parts A and B. Amsterdam, The Netherlands: ASMEDC, 2002, 5: 411-420.

[23] WANG Wei. The effects and flow mechanisms of tip injection and recirculating casing treatment in axial flow compressors[D]. Xi'an, China: Northwestern Polytechnical University, 2016.(in Chinese)

[24] YAN Song, CHU Wuli. Effect of self-circulating treatment casing on rotor performance at different speeds[J]. Journal of Aerospace Power, 2019, 34(11): 2516-2528. (in Chinese)

[25] YAN S, CHU W L. The improvement of transonic compressor performance by the self-circulating casing treatment[J]. Journal of Mechanical Engineering Science, 2021, 235(7): 1165-1176.

[26] ZHOU Hai, LI Qiushi, LU Yajun. Prospects of numerical analysis of an aspirated transonic fan rotor[J]. Journal of Aerospace Power, 2004, 19(3): 408-412. (in Chinese)

[27] BAI Meng, JIN Hailiang, JIN Donghai, et al. Numerical research on the influence of boundary layer suction on the stall margin of a high loading transonic two-stage fan[J]. Gas Turbine Experiment and Research, 2012, 25(2): 12-17. (in Chinese)

[28] LIU Bao, DU Zhengshuai, ZHOU Xun. Influence of endwall suction slot arrangement on performance of the aspirated compressor plane cascade[J]. Journal of Experiments in Fluid Mechanics, 2022, 36(4): 84-93. (in Chinese)

[29] LIU Taiqiu, WANG Jiayu, LI Lili. Thinking on aero-

dynamic design for highly-loaded compressors[J]. Aerospace Power, 2023, (6): 61-64. (in Chinese)

[30] YIN Song, GUO Haining, WEI Lai, et al. Refined design of highly loaded compressor[J]. Aeroengine, 2023, 49(5): 129-135. (in Chinese)

[31] DU J, LI F, LI J C, et al. A study of performance and flow mechanism of a slot-groove hybrid casing treatment in a low-speed compressor[C]//Proceedings of Volume 2C: Turbomachinery. Montreal, Canada: American Society of Mechanical Engineers, 2015: V02CT44A029.

[32] LI J C, DU J, LI F, et al. Stability enhancement using a new hybrid casing treatment in an axial flow compressor[J]. Aerospace Science and Technology, 2019, 85: 305-319.

[33] LIU W H, CHU W L, ZHANG H G. Stability improvement with slot-groove hybrid casing treatment in a high-speed axial compressor[J]. International Journal of Aeronautical and Space Sciences, 2025, 26 (5): 2226-2242.

[34] WANG Wei, CHU Wuli, ZHANG Haoguang. Study of design of a coupled casing treatment for a two-stage high-loaded axial flow compressor[J]. Journal of Propulsion Technology, 2017, 38(10): 2365-2373. (in Chinese)

[35] ZHANG Guochen, ZHANG Chengfeng, CAO Zhiyuan, et al. Numerical study on coupling of blade slotting and boundary layer suction to control compressor stall margin[J]. Journal of Propulsion Technology, 2023, 44(1): 121-129. (in Chinese)

Author

The first author Mr. **MENG Dejun** obtained his master's degree in engineering from Beihang University in 2011. He is a senior researcher and deputy chief engineer. His main research field is the aerodynamic design of compressor.

The corresponding author Ms. **LIU Jie** obtained her master's degree in engineering from Harbin Institute of Technology in 2008. Her main research field is the aerodynamic design of compressor.

Author contributions Mr. **MENG Dejun** designed the study, performed the numerical simulation, conducted the analysis, interpreted the results and wrote the manuscript. Mr. **YIN Haibao** contributed to the discussion and background of the study. Mrs. **LIU Jie** contributed to the data processing and analysis, and refined the manuscript and revised the paper according to the reviewers' comments. All authors commented on the manuscript draft and approved the submission.

Competing interests The authors declare no competing interests.

(Production Editor: WANG Jie)

耦合流动控制方法改善高负荷轴流压气机稳定性

孟德君，尹海宝，刘 杰

（中国航空发动机集团有限公司沈阳发动机研究所，沈阳 110015，中国）

摘要：为解决转子和静子流动失稳几乎同时触发条件下高负荷轴流压气机常规扩稳手段效果有限的问题，以某高负荷轴流压气机为研究对象，开展转静子耦合流动控制方法及其扩稳机理研究。首先，通过分析压气机失稳过程中的内部流场结构，揭示了该压气机流动失稳主要由转子叶顶区域流动堵塞和静子近轮毂区域流动堵塞共同诱发。随后，分别研究了自循环机匣处理、轮毂抽吸以及二者耦合控制方案对压气机内部流动结构和稳定性的影响。结果表明，自循环机匣处理能够改善转子叶顶区域的流通能力，但由于静子近轮毂区域流动堵塞未得到有效抑制，轮毂区域流场更易率先崩溃并触发压气机失稳，因此其失速裕度提升效果有限；轮毂抽吸能够显著改善静子近轮毂区域流场，但因未能有效抑制转子叶顶区域流动堵塞，其扩稳能力同样受限。进一步将自循环机匣处理与轮毂抽吸相结合后，耦合流动控制方法能够同时改善转子叶顶区域和静子近轮毂区域的流动状态，协同抑制两类关键堵塞结构的发展，从而显著拓宽压气机稳定工作范围。采用该耦合流动控制方法后，压气机失速裕度提高了6.78%。研究结果表明，对于转静子流动失稳耦合触发的高负荷轴流压气机，仅针对单一失稳源的控制方法难以获得理想扩稳效果，而面向多失稳源协同抑制的耦合流动控制方法是提升压气机稳定性的有效途径。

关键词：轴流压气机；高负荷；稳定性；耦合流动控制方法；流动机理

研究亮点：

1. 揭示了高负荷轴流压气机流动失稳由转子叶顶流动堵塞和静子近轮毂流动堵塞共同诱发的流动机理。
2. 对比分析了自循环机匣处理、轮毂抽吸及其耦合控制方法对压气机稳定性的影响规律。
3. 提出了一种转静子耦合流动控制方法，实现了对转子叶顶和静子近轮毂关键堵塞区域的协同抑制。采用耦合流动控制方法后，压气机失速裕度提高了6.78%，验证了该方法的有效性。